MCB
Journals.ASM.org

Interaction of PDK1 with Phosphoinositides Is Essential for Neuronal Differentiation but Dispensable for Neuronal Survival

Tinatin Zurashvili,[a] Lluís Cordón-Barris,[a] Gerard Ruiz-Babot,[a] Xiangyu Zhou,[a] Jose M. Lizcano,[a] Nestor Gómez,[a] Lydia Giménez-Llort,[b] Jose R. Bayascas[a]

Institut de Neurociències and Departament de Bioquímica i Biologia Molecular, Universitat Autònoma de Barcelona, Barcelona, Spain[a]; Institut de Neurociències and Departament de Psiquiatria i de Medicina Legal, Universitat Autònoma de Barcelona, Barcelona, Spain[b]

3-Phosphoinositide-dependent protein kinase 1 (PDK1) operates in cells in response to phosphoinositide 3-kinase activation and phosphatidylinositol-3,4,5-trisphosphate [PtdIns(3,4,5)P_3] production by activating a number of AGC kinases, including protein kinase B (PKB)/Akt. Both PDK1 and PKB contain pleckstrin homology (PH) domains that interact with the PtdIns(3,4,5)P_3 second messenger. Disrupting the interaction of the PDK1 PH domain with phosphoinositides by expressing the PDK1 K465E knock-in mutation resulted in mice with reduced PKB activation. We explored the physiological consequences of this biochemical lesion in the central nervous system. The PDK1 knock-in mice displayed a reduced brain size due to a reduction in neuronal cell size rather than cell number. Reduced BDNF-induced phosphorylation of PKB at Thr308, the PDK1 site, was observed in the mutant neurons, which was not rate limiting for the phosphorylation of those PKB substrates governing neuronal survival and apoptosis, such as FOXO1 or glycogen synthase kinase 3 (GSK3). Accordingly, the integrity of the PDK1 PH domain was not essential to support the survival of different embryonic neuronal populations analyzed. In contrast, PKB-mediated phosphorylation of PRAS40 and TSC2, allowing optimal mTORC1 activation and brain-specific kinase (BRSK) protein synthesis, was markedly reduced in the mutant mice, leading to impaired neuronal growth and differentiation.

During the development of the nervous system, among all the neuronal precursors initially produced during the neurogenesis stage, only those encountering the appropriate set of neurotrophic factors along with a complex set of extracellular positional signals will be further selected to survive and differentiate (1). The phosphoinositide 3-kinase (PI3K)/protein kinase B (PKB) axis is one of the critical intracellular signaling pathways that promotes neuronal survival by inhibiting the apoptotic cell death machinery in response to a number of extracellular stimuli (2). Thus, pharmacological inhibition of PI3K catalytic activity causes neuronal cell death, while forced expression of constitutively active forms of the PKB/Akt kinase promotes the survival of many neuronal cell types (3). PI3K also plays fundamental roles in regulating neuronal differentiation by defining the axon-dendrite axis through the activation of PKB (4). PKB promotes axon specification by inhibiting glycogen synthase kinase 3β (GSK3β) (5). PKB also inhibits the TSC1-TSC2 complex, which antagonizes axon formation by inhibiting mTORC1 and in this way restricting the expression of the brain-specific kinase (BRSK)/SAD kinases (6), which are known to play fundamental roles in neuronal polarization *in vivo* (7, 8).

However, mice lacking the neuronal Akt3/PKBγ isoform are viable and do not exhibit any overt phenotype, although they display a reduced brain size, with neurons more sensitive to apoptotic insults (9, 10). Therefore, the contribution of kinases activated downstream of the PI3K cascade besides PKB cannot be overlooked. In this regard, a role for the closely related kinase serum- and glucocorticoid-induced kinase (SGK) (11) or p90 ribosomal S6 kinase (RSK) (12) in promoting neuronal survival, and for RSK in promoting neurite outgrowth (13), has also been proposed.

3-Phosphoinositide-dependent protein kinase 1 (PDK1) elicits cellular responses to growth factors, hormones, and many other agonists that signal through PI3K activation and phosphatidylinositol-3,4,5-trisphosphate [PtdIns(3,4,5)P_3] production by directly activating as many as 23 protein kinases of the AGC family. These protein kinases include PKB/Akt, p70 ribosomal S6 kinase (S6K), SGK, RSK, and protein kinase C (PKC) isoforms, which in turn regulate cell growth, proliferation, survival, as well as metabolism (14, 15). All these AGC kinases share structural homology and a common mechanism of activation based on the dual phosphorylation of two residues lying within two highly conserved motifs, namely, the T loop (Thr308 residue for PKBα) and the hydrophobic motif (Ser473 residue for PKBα). PDK1 acts as the master upstream kinase activating this set of AGC kinases by phosphorylating their T-loop sites (16). The hydrophobic motif kinase is different among the different AGC family members, although a prominent role for mTOR complexes has emerged (17). Thus, the mTORC1 complex phosphorylates the hydrophobic motif of S6K isoforms (18, 19) and novel PKC isoforms (20), while the mTORC2 complex is the hydrophobic motif kinase for PKB (21), PKCα (22), and SGK (23) isoforms.

PDK1 is expressed in cells as a constitutively active enzyme which is not modulated by any stimuli. Regulation of this intricate signaling network relies instead on the ability of PDK1 to specifically recognize and interact with its substrates (24). The interaction of PDK1 with most AGC kinases needs the previous phosphorylation of their hydrophobic motifs, which in this manner become a substrate docking site for PDK1 binding (25). Activa-

Received 1 August 2012 **Returned for modification** 28 August 2012
Accepted 19 December 2012
Published ahead of print 28 December 2012
Address correspondence to Jose R. Bayascas, joseramon.bayascas@uab.cat.

doi:10.1128/MCB.01052-12

tion of PKB/Akt isoforms represents an exception to this general mechanism. Among all the PDK1-activated kinases, PKB isoforms are the only ones possessing pleckstrin homology domains, a phosphoinositide binding domain that is also present in the PDK1 protein (26, 27). The specific binding of the pleckstrin homology domain of PKB with PtdIns(3,4,5)P_3 becomes rate limiting for the translocation of PKB to the plasma membrane and colocalization with PDK1, where PDK1 can then efficiently phosphorylate PKB at Thr308 (28, 29), while mTORC2 phosphorylates the Ser473 site in the hydrophobic motif (21), resulting in maximal activation of the enzyme. The significance of the interaction of the PDK1 PH domain with phosphoinositides in the activation of PKB has been evaluated *in vivo* using PDK1$^{K465E/K465E}$ knock-in mice (30), which express a rationally designed point mutant form of PDK1 that retains catalytic activity but is incapable of phosphoinositide binding (27). In tissues derived from these mice, PKB is still activated by growth factors albeit to a reduced level (30–32), whereas the activation of the rest of the PDK1 substrates proceeds normally. As a consequence, these mice are smaller, prone to diabetes (30), and protected from PTEN-induced tumorigenesis (32). The PDK1$^{K465E/K465E}$ mouse is a genuine model in which PKB activation is only moderately reduced, which might originate from the ability of PDK1 to recognize the PKB Ser473 phospho-docking site in the absence of phosphoinositide binding (33). This genetic model has proven instrumental in dissecting PDK1 signaling (34) and has revealed that in T cells a PKB/Akt signaling threshold depending on PDK1-phosphoinositide interactions dictates specific cellular responses such as cell migration but not cell proliferation (31).

In the present study, we have employed PDK1$^{K465E/K465E}$ knock-in mice to explore the role that the interaction of the PDK1 PH domain with phosphoinositides plays in neuronal tissues. We found that the brain of homozygous PDK1$^{K465E/K465E}$ knock-in mice was reduced in size due to a reduction in cell size rather than cell number. In agreement with the maintenance of the number of cells, both the sensitivity of the mutant neurons to apoptosis induced by serum withdrawal as well as the ability of different growth factors to support neuronal survival in the absence of serum were preserved in the mutant neurons. The deficient activation of PKB and incomplete phosphorylation and inactivation of PRAS40 and TSC2 observed in the mutant neurons caused decreased mTORC1 activation, leading to reduced BRSK protein synthesis and deficient neuronal differentiation.

MATERIALS AND METHODS

Materials and constructs. Protease inhibitor cocktail, thiazolyl blue tetrazolium bromide [3-(4,5-dimethylthiazol-2-yl)-2,5-diphenyltetrazolium bromide (MTT)], staurosporine, Dulbecco's modified Eagle's medium (DMEM), basal medium Eagle (BME), and fetal bovine serum (FBS) were purchased from Sigma. Human recombinant BDNF was obtained from Alomone, and human recombinant IGF-1 was obtained from Millipore. The Calbiochem inhibitors Akti-1/2 (catalog number 124018), PI-103 (catalog number 528100), rapamycin (catalog number 553210), and SB-216763 (catalog number 361566) were purchased from Merck Millipore. Neurobasal medium, B27 supplement, Opti-MEM, and Lipofectamine 2000 were obtained from Invitrogen. Hemagglutinin (HA)-tagged human BRSK1 and BRSK2 (35) were subcloned into a pEIGW lentiviral vector that allows the expression of both green fluorescent protein (GFP) and BRSK1/2 from a bicistronic messenger.

Antibodies. The following antibodies were kindly provided by Dario Alessi from the University of Dundee. All antibodies were raised in sheep and affinity purified on the appropriate antigen. The PKBα total antibody was raised against the sequence RPHFPQFSYSASGTA, corresponding to residues 466 to 480 of rat PKBα; the total TSC2 antibody was raised against a sequence encompassing residues 1719 to 1814 of mouse TSC2; the total PRAS40 antibody was raised against the peptide DLPRPRLNTS DFQKLKRKY, corresponding to residues 238 to 256 of human PRAS40; and the total NDRG1 antibody was raised against the recombinant human NDRG1 protein expressed in *Escherichia coli*. Affinity-purified polyclonal BRSK1- or BRSK2-specific antibodies were raised in sheep against the peptide SPRRGPPKDKKLLATNGTPLP, corresponding to C-terminal residues 774 to 794 of human BRSK1, and the peptide LSWGAGLKGQK VATSYESSL, encompassing residues 655 to 674 of human BRSK2, as described previously (36). Phospho-PKB Thr308 (catalog number 9275), phospho-PKB Ser473 (catalog number 9271), phospho-S6K Thr389 (catalog number 9205), total S6K (catalog number 9202), phospho-S6 ribosomal protein Ser235/236 (catalog number 2211), total S6 ribosomal protein (catalog number 2217), phospho-p44/42 mitogen-activated protein kinase (MAPK) Thr202/Tyr204 (catalog number 9101), total p44/42 MAPK (catalog number 9102), phospho-GSK3α/β Ser21/9 (catalog number 9331), phospho-FOXO1 Ser256 (catalog number 9461), phospho-FOXO1 Thr24 (catalog number 9464), total FOXO1 (catalog number 2880), phospho-RSK Ser380 (catalog number 9335), phospho-RSK Thr573 (catalog number 9346), total RSK1/2/3 (catalog number 9355), phospho-TSC2 Thr1462 (catalog number 3611), phospho-PRAS40 Thr246 (catalog number 2997), phospho-NDRG1 Thr346 (catalog number 5482), phospho-TrkB Tyr706/707 (catalog number 4621), and total TrkB (catalog number 4603) antibodies were purchased from Cell Signaling Technology. The pan-PDK1 site antibody from Cell Signaling Technology (catalog number 9379) recognizes phosphorylated Thr229 of S6K in cell extracts (37). Total GSK3α/β (sc-7291) and phospho-RSK Thr227 (sc-12445) antibodies were purchased from Santa Cruz Biotechnology. Appropriate secondary antibodies coupled to horseradish peroxidase were obtained from Pierce. For the immunofluorescence analysis, the anti-Tau-1 monoclonal antibody (MAB3420) was purchased from Millipore, the pan-axonal anti-neurofilament H monoclonal antibody (SMI-312R) was obtained from Covance, and the rabbit anti-MAP2 polyclonal antibody (M3696) was obtained from Sigma; Alexa Fluor 594-conjugated goat anti-rabbit (catalog number A11072) and Alexa Fluor 488-conjugated goat anti-mouse (catalog number A11017) fluorescent secondary antibodies were obtained from Invitrogen.

Mice. The generation and genotyping of PDK1$^{K465E/K465E}$ knock-in mice expressing the single-amino-acid substitution of lysine 465 to glutamic acid in the PDK1 PH domain were described previously (30). Mice were maintained in the Animal House Facility of the Universitat de Lleida under standard husbandry conditions. All animal studies and breeding were approved by the Universitat Autònoma de Barcelona ethical committee and performed under a Generalitat de Catalunya project license.

Primary cultures. Cerebral cortical or hippocampal tissues were dissected from PDK1$^{+/+}$ and PDK1$^{K465E/K465E}$ littermate mice at embryonic day 15.5 (E15.5), and the cells were enzymatically dissociated in Krebs Ringer buffer (120 mM NaCl, 4.8 mM KCl, 1.2 mM KH_2PO_4, 25 mM $NaHCO_3$, 14.3 mM glucose) containing 0.25 mg/ml of trypsin for 10 min at 37°C and were then mechanically dissociated in Krebs Ringer buffer containing 0.08 mg/ml DNase and 0.52 mg/ml trypsin inhibitor by gentle pipetting using a fire-polished Pasteur pipette to produce a single-cell suspension. Cells were then centrifuged and resuspended, counted with the Scepter 2.0 handheld automated cell counter (Millipore), and finally diluted in DMEM complemented with 2 mM L-glutamine, 0.25 mg/ml penicillin-streptomycin, and 10% FBS. The cortical cells were then plated onto poly-D-lysine (50 μg/ml)-coated 24-well plates for cell viability studies, or 6-well plates for Western blot analysis, at a density of 15×10^4 cells/ml, whereas the hippocampal cells were plated onto poly-D-lysine (150 μg/ml)-coated 12-mm-diameter glass coverslips at a density of 5×10^4 cells/ml. The cells were allowed to attach to the plate for 2 h, and the medium was then replaced by Neurobasal medium complemented with 2

mM L-glutamine, 0.25 mg/ml of penicillin-streptomycin, and 2% B27 supplement. Cells were maintained at 37°C in a humidified incubator containing 5% CO_2 under normoxia conditions.

Cerebellar granule cell cultures were prepared from dissociated cerebella of 8-day-old mice by mechanically chopping the cerebellum, followed by trypsin digestion and triturating, as described above. Cells were plated onto BME supplemented with 25 mM KCl, 10% FBS, and 0.25 mg/ml of penicillin-streptomycin. Cytosine-β-D-arabinofuranoside (10 μM) was added to the culture after 24 h of seeding to prevent the proliferation of nonneuronal cells. Cells were plated onto 48-well culture plates coated with 10 μg/ml poly-L-lysine at a density of 1.35×10^6 cells/ml.

Trophic deprivation and drug treatment. Survival experiments were performed at day 6 *in vitro* (DIV6). Cells were washed twice with serum-free DMEM and then incubated for 24 h in serum-free Neurobasal medium supplemented with 2 mM L-glutamine and 0.25 mg/ml of penicillin-streptomycin. The experimental controls included sham treatments consisting of two washes with serum-free medium and incubation with the same conditioned medium. BDNF and IGF-1 were diluted in DMEM without any supplement. The inhibitors Akti-1/2, PI-103, SB-216763, staurosporine, and rapamycin were dissolved in dimethyl sulfoxide (DMSO). For viability and apoptosis analysis, growth factors and inhibitors were added at the onset of trophic deprivation. For Western blot analysis, cells were pretreated with inhibitors for 30 min and then stimulated with BDNF, as indicated.

Evaluation of cell viability. Cell viability was determined by an MTT reduction assay. Briefly, MTT salt was added to the cell culture at a final concentration of 0.5 mg/ml. Plates were then returned to the incubator for 45 min. After incubation, the medium was aspirated, and the resulting formazan crystals were dissolved by mixing with 300 μl of DMSO. Absorbance intensity was measured at 570 nm, with the background measured at 690 nm, using a spectrophotometer running Labsystem Multiskan software.

Quantification of apoptosis. Cells were fixed in 2% paraformaldehyde, stained with 1 μg/ml of the DNA dye Hoechst 33342, and then visualized under a fluorescence microscope. Apoptosis was quantified at each condition point by scoring the percentage of apoptotic cells in the adherent cell population. Cells exhibiting fragmented or condensed nuclei were scored as apoptotic, while cells showing uniformly stained nuclei were scored as viable. At least 300 cells from 6 randomly selected fields per well were counted.

Transfection. A total of 2.5×10^4 embryonic hippocampal neurons grown for 2 days in 12-mm-diameter 24-well plates were transfected with 0.7 μl of Lipofectamine 2000 reagent diluted in 50 μl of Opti-MEM plus 1 μg of the indicated DNA diluted again in 50 μl of Opti-MEM. After 3 h, the transfection medium was replaced by conditioned medium, and the axon length of the GFP-expressing cells was evaluated at day 4 *in vitro*, as described above.

Generation of protein extracts and Western blot analysis. Primary cortical neurons were cultured for 6 days and then incubated for 4 h in Neurobasal medium without B27 and subsequently stimulated with the indicated agonists, as described in the figure legends. The neurons were lysed at the indicated time points in ice-cold lysis buffer (50 mM Tris-HCl [pH 7.5], 1 mM EGTA, 1 mM EDTA, 1 mM sodium orthovanadate, 50 mM sodium fluoride, 5 mM sodium pyrophosphate, 10 mM sodium β-glycerophosphate, 0.27 M sucrose, 1% [wt/vol] Triton X-100, 0.1% [vol/vol] 2-mercaptoethanol, and a 1:100 dilution of protease inhibitor cocktail) and centrifuged at 4°C for 10 min at 13,000 × *g*. Tissue extracts were prepared by homogenizing the frozen tissue on ice in a 10-fold excess volume of ice-cold lysis buffer using the Polytron homogenizer and then centrifuged at 4°C for 10 min at 13,000 × *g* to remove insoluble material. The supernatants were aliquoted, frozen in liquid nitrogen, and stored at −20°C until use. Protein concentrations were determined by the Bradford method (38), using bovine serum albumin (BSA) as a standard. The activation state of the different pathways analyzed was assessed by immunoblotting the extracts (10 μg) with the indicated antibodies and detected with the appropriate horseradish peroxidase-conjugated secondary antibodies. Membranes were incubated with enhanced chemiluminescence (ECL) reagent, either exposed to Super RX Fujifilm and developed or detected by using a GeneGnome HR detection system (Syngene, Cambridge, United Kingdom), and quantified by using ImageJ software.

Determination of organ volume and cell size. Organ volume was determined by using the Cavalieri method (39) on 8-μm brain paraffin sections collected at systematically spaced locations ($k = 96$ μm) from a random starting position. The sections were photographed with a Nikon SMZ800 stereomicroscope at a ×2 magnification using a digital camera. A square lattice grid was then overlaid onto the picture by using the program Photoshop, version vCS5.1, and the number of intersections (P) hitting the organ was scored. The organ volume was then estimated by using the equation $\Sigma P \times d^2 \times k$, in which d^2, the distance between each point of the square lattice grid squared, was 0.14792 mm^2. The number and size of the cells in E15.5 dissociated cortex and hippocampal tissues were determined with the Scepter 2.0 handheld automated cell counter (Millipore).

Immunocytochemistry. Dissociated hippocampal cells were cultured on coverslips for the indicated number of experimental days *in vitro* and then fixed with 4% paraformaldehyde in phosphate-buffered saline (PBS) for 20 min at room temperature. Fixative solution was rinsed 3 times with PBS for 5 min, and the cells were then permeabilized with 0.02% saponin in PBS for 7 min at room temperature and blocked in a solution containing 0.01% saponin, 5% BSA, and 10 mM glycine in PBS for 1 h. Primary antibodies were diluted 1:200 in PBS supplemented with 0.01% saponin and 1% normal goat serum and incubated overnight at 4°C. Cells were then washed three times with PBS for 10 min. Appropriate secondary antibodies conjugated to Alexa Fluor 594 or Alexa Fluor 488 fluorescent dye were used at a concentration of 1:400, and nuclei were stained with 1 μg/ml Hoechst 33342. Coverslips were then mounted onto microscope slides with FluorSave reagent for further analysis.

Immunohistochemistry. Three $PDK1^{+/+}$ and three $PDK1^{K465E/K465E}$ matched littermate mice were anesthetized by intraperitoneal injection of a ketamine-xylazine mixture and then intracardially perfused with 0.9% NaCl followed by 4% buffered paraformaldehyde. Brains were extracted and postfixed with the same solution for 2 h, washed in phosphate buffer (0.1 M, pH 6.0) for 2 h, and preserved in a 70% ethanol solution at 4°C. All six specimens were then embedded in the same paraffin block and sliced into 5-μm-thick coronal sections with a Leica RM2255 microtome. Paraffin-embedded sections were incubated for 2 h at 60°C and then rehydrated through a series of 2 washes with xylene for 5 min, 2 washes with 100% ethanol for 3 min, 1 wash with 96% ethanol for 3 min, 1 wash with 70% ethanol for 3 min, 1 wash with 50% ethanol for 5 min, and 1 wash with water for 1 min. Sections were then boiled for 10 min in 10 mM sodium citrate (pH 6) for antigen retrieval and cooled down for 30 min on ice. Samples were blocked in Tris-buffered saline (TBS) (50 mM Tris [pH 7.5], 150 mM NaCl) containing 0.02% Triton and 5% goat serum for 30 min and incubated overnight at 4°C with primary antibodies diluted in the same blocking solution (1:300 dilution for the rabbit anti-MAP2 antibody and 1:2,000 for the mouse monoclonal anti-pan-axonal marker SMI-312R). Sections were rinsed with TBS buffer and detected with Alexa Fluor 488-conjugated anti-mouse (dilution, 1:400) and Alexa Fluor 594-conjugated anti-rabbit (1:300) secondary antibodies for 1.5 h at room temperature. Tissue autofluorescence was removed by incubation with Sudan Black for 10 min (0.3% [wt/vol] Sudan Black in 70% ethanol). Sections were counterstained with Hoechst dye and mounted with FluorSave reagent. Immunostained sections were photographed with a Nikon Eclipse 90i epifluorescence microscope, and the captured images were analyzed and processed with ImageJ 1.42q (Wayne Rasband, National Institutes of Health) and Fiji (http://pacific.mpi-cbg.de/wiki/index.php/Main_Page) software.

Evaluation of differentiation. For differentiation analysis of the cortical neurons, cells were seeded at a reduced density of 75,000 cells/ml. Under this condition, most neurons did not contact neighboring cells,

allowing the measurement of neurite development of individual neurons. Images were acquired from random fields at a ×20 magnification by using an inverted microscope equipped with a Hamamatsu Orca-Er high-sensibility camera at the maximal resolution of the microscope. The total neurite length per cell was measured by tracing all the neurites on each individual neuron from the cell body to the tip with Adobe Photoshop, version vCS5.1, software, and the number of pixels was converted to micrometers. The cell diameter was defined by using the same technique, by measuring the major axis of the neuronal cell body. The number of neurites per cell and the number of branching points per neurite were also determined by direct counting on the acquired images.

For differentiation analysis of hippocampal cells, images were obtained with an epifluorescence microscope (Nikon Eclipse 90i) interfaced with a DXM 1200F camera at a ×20 magnification. Images for the red and green channels were taken simultaneously. Neuronal dendrites were identified by immunostaining with the dendritic marker MAP2, whereas the axon was defined as a neurite whose length is 2 times longer than that of the other neurites and is also immunoreactive for the axonal marker Tau-1. To measure axonal elongation, each particular axon was manually traced, followed by automatic length calculation with MetaMorph image analysis software, v6.1.

Statistical analysis. Statistical significance was determined by using Student *t* test analysis. *P* values of <0.05 and <0.005 between categories or conditions are indicated in the figures.

RESULTS

Reduced brain size of PDK1$^{K465E/K465E}$ mice. Mice homozygous for the PDK1 K465E knock-in alleles were previously reported to be viable, fertile, and healthy, although they displayed a 35% reduction in body weight compared to wild-type mice (30). We observed the homozygous PDK1$^{K465E/K465E}$ genotype at a reduced Mendelian distribution from heterozygous crosses, both at embryonic day 15 and at birth (19.8% and 16.0%, respectively), thereby indicating that the PDK1 K465E mutation resulted in partial embryonic lethality (Fig. 1A). The growth deficiency of the PDK1$^{K465E/K465E}$ mice might initiate early during development, as we observed that at E15.5, the PDK1 knock-in embryos were already 20% smaller than their control littermates (Fig. 1B), with brain size also reduced to scale (Fig. 1C). The small phenotype was further exacerbated after the second week of age, as the body weight of the PDK1$^{K465E/K465E}$ mice was 30 to 35% reduced compared to that of the PDK1$^{+/+}$ mice from 3 weeks of age (Fig. 1B) and during their adulthood (data not shown). To establish whether the reduction in the embryonic brain volume could be attributed to a reduction in cell size or number, the volume of the neuronal soma and the number of neuronal cells purified at E15.5 from both the embryonic cortex and the hippocampus were determined. While the number of cortical and hippocampal neurons was not significantly different between genotypes, the soma was 20% reduced in volume in the cortical (Fig. 1D) and hippocampal (Fig. 1E) mutant cells compared to controls, thereby demonstrating that the small size of the PDK1$^{K465E/K465E}$ mouse brain is due mostly to a reduction in cell size rather than cell number.

Binding of PDK1 to PtdIns(3,4,5)P_3 is not essential to support neuronal survival. We next compared the protective effects that BDNF elicited on the survival of PDK1$^{+/+}$ and PDK1$^{K465E/K465E}$ cortical neurons deprived of growth factors. In control cultures, trophic factor deprivation compromised cell viability, as denoted by a 50% decrease in the MTT reduction values, which was accompanied by a 3-fold increase in the number of apoptotic cells compared to that in the untreated cultures. BDNF stimulation markedly recovered cell viability and decreased the number of apoptotic dying cells of the serum-deprived cortical cultures (Fig. 2A). Unexpectedly, trophic factor withdrawal compromised neuronal viability to the same extent in the PDK1$^{+/+}$ and the PDK1$^{K465E/K465E}$ cultures, which was equally rescued by BDNF treatment for the two genotypes, thereby suggesting that the interaction of PDK1 with phosphoinositides is not essential for the neuroprotective actions of BDNF, at least in cortical neurons. We extended our observations to other neuronal populations and found that IGF-1 prompted the survival of cerebellar granule cells deprived of serum and potassium to the same level in the PDK1$^{+/+}$ and the PDK1$^{K465E/K465E}$ cultures (Fig. 2B). Moreover, the PDK1$^{+/+}$ and the PDK1$^{K465E/K465E}$ cortical neurons exhibited the same sensitivity to apoptotic stimuli such as staurosporine (Fig. 2C). We also cultured cortical neurons in the presence of suboptimal doses of either BDNF or IGF-1 and found that the two trophic factors elicited a dose-dependent neuroprotective action that was similar in both control and mutant cultures (Fig. 2D). Because the interaction of PDK1 with phosphoinositides is important for PKB activation (30), and PKB/Akt is a major regulator of neuronal survival (2), but the neuronal survival responses were still not affected in the PDK1$^{K465E/K465E}$ mice (Fig. 2), we assessed whether inhibition of PKB compromised the protective role of BDNF against serum deprivation. To that end, we employed the inhibitor Akti-1/2, which specifically targets PKBα and PKBβ. The treatment of cortical cultures with the Akti-1/2 compound at specific doses that markedly prevented PKB phosphorylation at both the Thr308 and Ser473 sites did not affect the survival responses elicited by BDNF. As a control, cortical cultures were also treated with the PI3K-specific inhibitor PI-103, and we found that the inhibition of PI3K totally abolished both the recovery of cell viability and the inhibition of apoptosis induced by BDNF (Fig. 3).

Mutation of the PDK1 PH domain impairs BDNF-mediated PKB activation. To define the importance of the PDK1-PtdIns(3,4,5)P_3 interaction in the ability of PDK1 to activate PKB, primary cultures of cortical neurons derived from littermate PDK1$^{+/+}$ and PDK1$^{K465E/K465E}$ embryos were stimulated with BDNF for the indicated times (Fig. 4A). As a control for stimulation, the activation of the BDNF receptor TrkB was monitored by measuring its phosphorylation at the activation loop residues Tyr706/707, which was very rapid and sustained in both control and mutant cell extracts. In PDK1$^{+/+}$ cells, BDNF induced a clear activation of PKB, as judged by the level of phosphorylation of the two activating residues, Thr308 and Ser473, which reached the maximum after 5 min and was then sustained for up to 30 min. In contrast, the phosphorylation of PKB at Thr308, the PDK1 site, was significantly reduced in the PDK1$^{K465E/K465E}$ mutant neurons during the first 15 min of stimulation and was then detected at nearly normal levels after 30 min, whereas the phosphorylation of PKB at Ser473, the mTORC2 site, was not affected in the mutant cells (Fig. 4A and C). Consistent with a reduction in the ability of the PDK1 K465E mutant protein to activate PKB, the phosphorylation levels of some PKB substrates at their specific PKB sites, namely, PRAS40 at Thr246 and TSC2 at Thr1462, were also significantly reduced in the mutant extracts. In contrast, the PKB-specific phosphorylation of GSK3α/β at Ser21/9 and FOXO1 at Thr24 and Ser256 was not affected by the PDK1 mutation (Fig. 4A). The moderate changes to the PKB downstream signaling pathways that the PDK1 PH domain mutation causes were

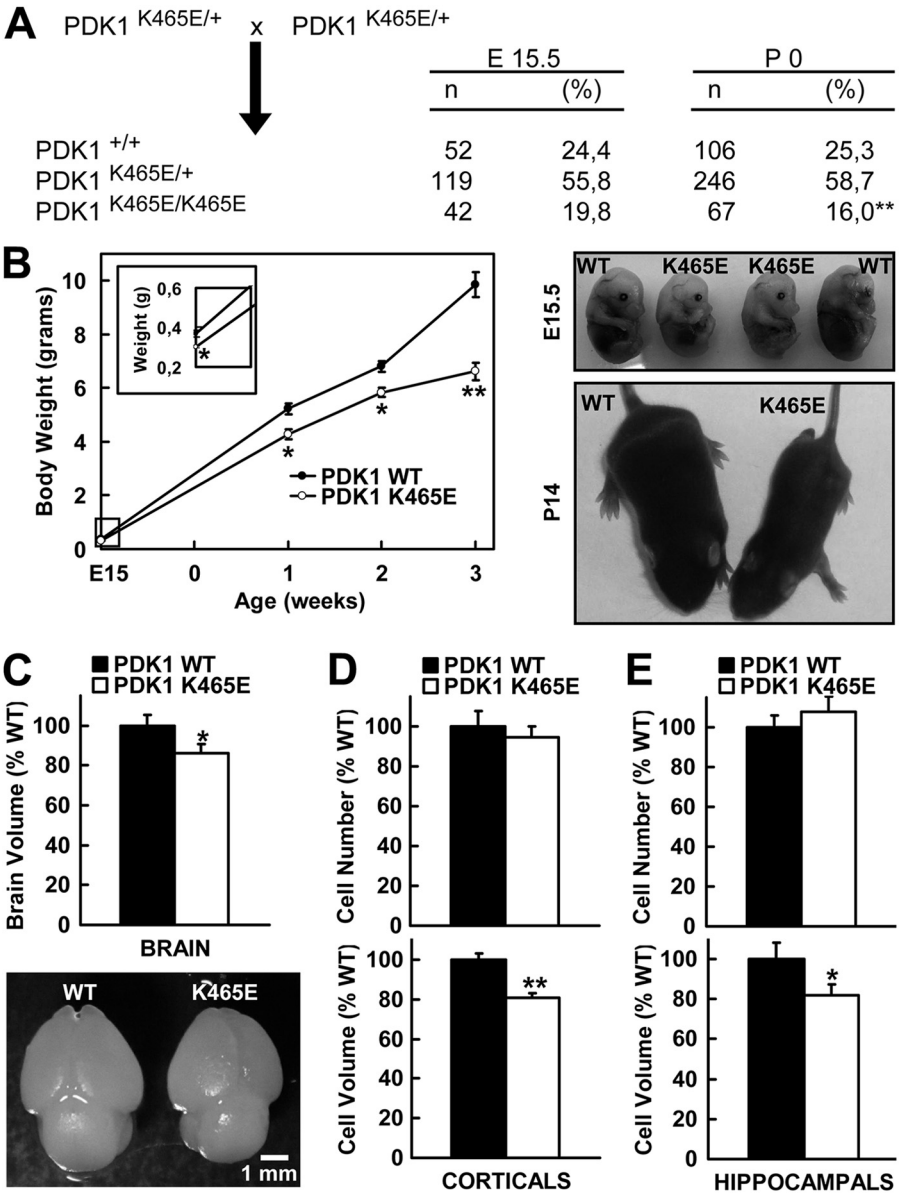

FIG 1 Reduced embryonic brain size in PDK1$^{K465E/K465E}$ mice. (A) The number and proportion (percentage) of mice of different genotypes resulting from heterozygous breeding are indicated both at embryonic day 15.5 (E15.5) and at birth (P0). ** indicates that the lower-than-expected frequency of PDK1$^{K465E/K465E}$ pups is statistically significant ($P < 0.005$ by χ^2 test). (B) The mean body weights of the indicated PDK1 wild-type (WT) and PDK1 K465E mice at the indicated ages in weeks are shown. The values represent the means ± standard errors of the means, with each data point obtained for at least five mice per genotype. Representative pictures of the indicated littermate PDK1 wild-type and PDK1 K465E embryos (E15.5) or 14-day-old pups (P14) are shown in the right panels. (C, top) The volume of the brain was measured at E15.5 from histological sections by using the Cavalieri method. The data are represented as the means ± standard errors of the means for three different mice per genotype. (Bottom) Representative photographs of brains dissected from E15.5 PDK1 wild-type and PDK1 K465E embryo littermates. Bar, 1 mm. (D and E) The number of cells (top) and the volume of the cell (bottom) were determined for E15.5 dissociated cortical (D) or hippocampal (E) neurons. The data are represented as the means ± standard errors of the means for 25 wild-type and 29 mutant embryonic cortical cultures obtained from 18 independent litters (D) or 8 wild-type and 7 mutant embryonic hippocampal cultures obtained from 6 independent litters (E). *, $P < 0.05$; **, $P < 0.005$ (compared with the wild type, as determined by the Student *t* test).

time and dose dependent and were better observed at low concentrations of BDNF (Fig. 4B).

Reduced activation of S6K in PDK1$^{K465E/K465E}$ cortical neurons. Activation of S6K involves the phosphorylation of the Thr389 residue within the S6K hydrophobic motif by mTORC1, followed by the phosphorylation of the Thr229 residue in the S6K activation loop by PDK1. Therefore, mTORC1 regulation greatly dictates S6K activation. PKB itself contributes to the activation of mTORC1 by phosphorylating and inhibiting two mTORC1-inhibitory proteins, namely, PRAS40 and TSC2. Accordingly, although S6K is a docking site-dependent PDK1 substrate, the reduced phosphorylation of PKB, PRAS40, and TSC2 proteins observed in the BDNF-stimulated PDK1$^{K465E/K465E}$ cortical neurons (Fig. 4) resulted in deficient activation of mTORC1, as

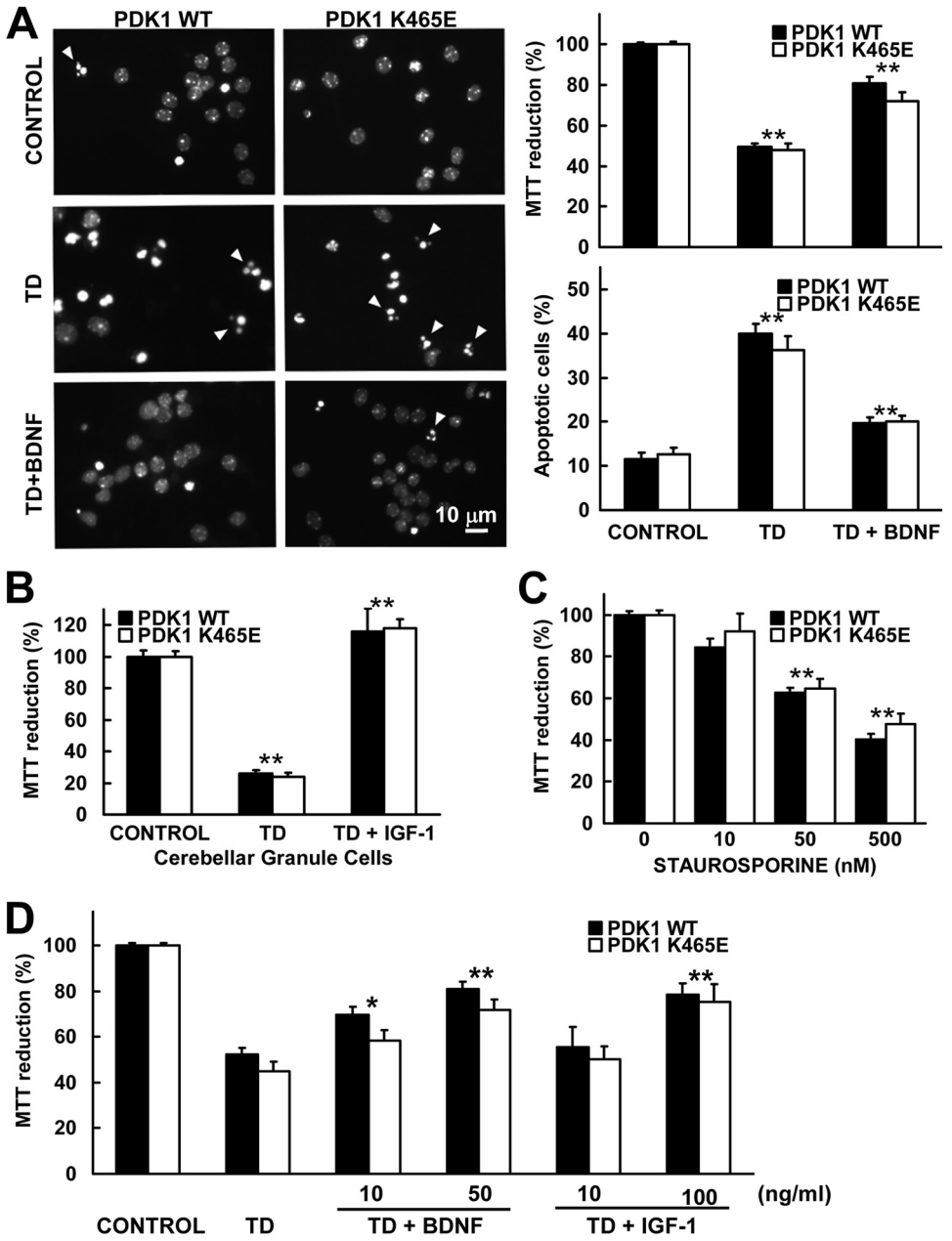

FIG 2 Neuronal survival responses are not impaired in PDK1$^{K465E/K465E}$ mice. (A) Cortical cells of the indicated genotypes were either sham treated (CONTROL) or deprived of trophic factors in the absence (TD) or presence of 50 ng/ml of BDNF (TD+BDNF) for 24 h. (Left) Representative micrographs of PDK1 wild-type (WT) and PDK1 K465E Hoechst-stained cortical neurons after 24 h of the indicated treatment; arrowheads indicate apoptotic nuclei. Bar, 10 μm. (Top right) Cell viability was determined with the MTT reduction assay and is expressed as a percentage of the untreated cells; data represent the means ± standard errors of the means for at least 20 independent mouse embryos per genotype from seven different litters, with each sample assayed in triplicate. (Bottom right) The percentage of apoptotic cells was obtained by scoring the number of nuclei exhibiting chromatin fragmentation divided by the total; data represent the means ± standard errors of the means for at least nine independent mouse embryos per genotype from four independent litters. (B) Cerebellar granule cells were either sham treated (CONTROL) or deprived of serum and potassium in the absence (TD) or presence of 100 ng/ml of IGF-1 (TD + IGF-1) for 24 h. Cell viability was measured, as described above for panel A, from three different mouse pups of each genotype assayed in quadruplicate. (C) Cortical cell cultures in complete medium were treated with the indicated doses of staurosporine for 24 h, and cell viability was then determined, as described above for panel A, from samples of at least seven independent embryos per genotype from four independent pregnancies, with each sample assayed in triplicate. (D) Cortical cells of the indicated genotypes were treated as described above for panel A, in the presence of the indicated concentrations of BDNF or IGF-1 for 24 h. Cell viability was determined from samples of at least five independent mouse embryos per genotype, with each sample assayed in triplicate. *, $P < 0.05$; **, $P < 0.005$ (between trophic deprivation and controls [A and B], BDNF or IGF-1 stimulation and trophic deprivation [A, B, and D], and staurosporine treatment and untreated controls [C], as determined by the Student *t* test).

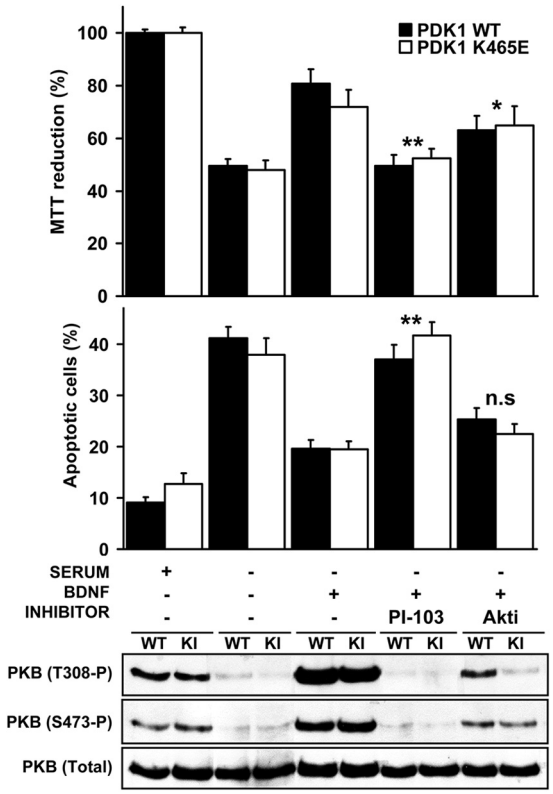

FIG 3 The PKB inhibitor Akti-1/2 does not impair neuronal survival. Cortical cells of the indicated genotypes were cultured in complete medium or deprived of serum for 24 h in the absence or presence of 50 ng/ml of BDNF, 1 μM PI-103, or 1 μM Akti-1/2, as indicated. MTT reduction and the percentage of apoptotic nuclei were determined and are represented as the means ± standard errors of the means for at least five independent embryos per genotype from two separate experiments, with each sample assayed in triplicate. As a control for the different treatments, cell lysates from matched PDK1 wild-type (WT) and PDK1 mutant (knock-in [KI]) littermate mice were immunoblotted with the indicated antibodies. n.s., not significant; *, $P < 0.05$; ** $P < 0.005$ (between samples treated with BDNF plus the indicated inhibitor and samples treated with BDNF alone, as determined by Student's *t* test).

judged by the reduced phosphorylation of S6K at Thr389, although this defect was very transient and detectable only at 5 min of BDNF treatment. As a consequence, PDK1 phosphorylation of the Thr229 residue was also reduced, leading to decreased S6K activation, as revealed by the impaired phosphorylation of the ribosomal S6 protein at Ser235 (Fig. 5A).

Normal activation of RSK in PDK1$^{K465E/K465E}$ neurons. RSK is activated downstream of the extracellular signal-regulated kinase (ERK) signaling pathway in a multistep phosphorylation sequence. ERK activates the C-terminal kinase domain (CTKD) of RSK by phosphorylating the T-loop Thr573 residue. Activated CTKD autophosphorylates the RSK hydrophobic motif at Ser380, thereby creating the docking site for PDK1, which can then phosphorylate the T-loop residue Ser227 in the N-terminal kinase domain (NTKD), leading to its activation (40). BDNF induced a rapid phosphorylation of ERK1/2 at Thr202/Tyr204 in cortical cells, which reached the maximum at 5 min and was sustained for 30 min. As expected, this was not affected by the PDK1 K465E mutation. This was accompanied by a robust induction of RSK phosphorylation at Thr573, Ser380, and Ser227, which was similar in both control and mutant cells (Fig. 5B).

Reduced phosphorylation of the SGK1 substrate NDRG1. Activation of SGK1 encompasses the phosphorylation of the hydrophobic motif at Ser422 by mTORC2, which primes the phosphorylation of the T loop at Thr256 by PDK1. The n-myc downstream-regulated gene (NDRG) family members were identified as the first specific physiological substrates of the SGK isoforms (41), and the phosphorylation of the NDRG1 protein at Thr346/356/366 sites, lying in a C-terminal decapeptide repeated sequence, is used as a readout of SGK1 activity (23). The NDRG proteins play important roles in the development of the central nervous system. Mutations in the NDRG1 gene cause motor and sensory neuropathy in humans (42), whereas NDRG1-deficient mice exhibited peripheral nerve degeneration (43). NDRG2 levels are upregulated in Alzheimer disease (44), and NDRG4-deficient mice exhibit spatial learning deficits and vulnerabilities to cerebral ischemia (45). However, the physiological relevance of NDRG phosphorylation by SGK1 in neurons is largely undefined. We used antibodies that recognize the phosphorylated C-tail repeats of the NDRG1 protein and found that BDNF rapidly induced the phosphorylation of NDRG1 at the SGK1 sites in PDK1$^{+/+}$ cortical neurons, which was significantly reduced in the PDK1$^{K465E/K465E}$ cells at 5 min of BDNF treatment (Fig. 6A). This observation was puzzling, because a role for the PDK1-phosphoinositide interaction in the activation of SGK1 could not be envisaged. Another scenario would be that the PKB isoforms contributed to the phosphorylation of NDRG1 at Thr346/356/366, at least in neurons. We tested this notion by stimulating cortical neurons with BDNF in the presence of the inhibitor Akti-1/2 and found that BDNF-induced phosphorylation of NDRG1 at Thr346/356/366 was greatly reduced by the Akti-1/2 compound at doses that did not affect other closely related kinases, such as RSK (Fig. 6B). Since SGK1 phosphorylation primes NDRG1 for GSK3 phosphorylation four amino acids N terminal to the residues phosphorylated by SGK1 (positions $n - 4$) (41), the phosphorylation of NDRG1 at Ser342/352/362 by GSK3, which could have been enhanced by the PDK1 K465E mutation, might have interfered with the recognition of NDRG1 by the phospho-Thr346/356/366 antibody. Treatment of BDNF-stimulated cells with two independent GSK3 inhibitors, namely, lithium and SB-216763, caused an increase in the electrophoretic mobility of the NDRG1 protein, which was compatible with a decrease in the abundance of the hyperphosphorylated NDRG1 species. In contrast, inhibitors of GSK3 did not significantly affect the intensity of the phospho-Thr346/356/366 signal (Fig. 6B), thereby indicating that the phosphorylation of the GSK3 sites was not masking the NDRG1 phospho-Thr346/356/366 antibody epitope and further suggesting a direct role of PKB in phosphorylating neuronal NDRG1 at the SGK1 sites.

PtdIns(3,4,5)P_3 binding to PDK1 promotes neuronal differentiation through the PKB/mTORC1/BRSK pathway. We showed that disruption of the interaction of PDK1 with PtdIns(3,4,5)P_3 in PDK1$^{K465E/K465E}$ mice affected the activation of PKB by BDNF, leading to the inhibition of the downstream mTORC1 and S6K signaling pathways. Since mTORC1 plays fundamental roles in regulating neuronal morphogenesis (46), we aimed to determine whether PDK1$^{K465E/K465E}$ mice exhibited alterations in neuronal morphology. To that end, primary cortical neurons derived from PDK1$^{+/+}$ and PDK1$^{K465E/K465E}$ E15.5 embryos were allowed to differentiate in culture, and the complexity

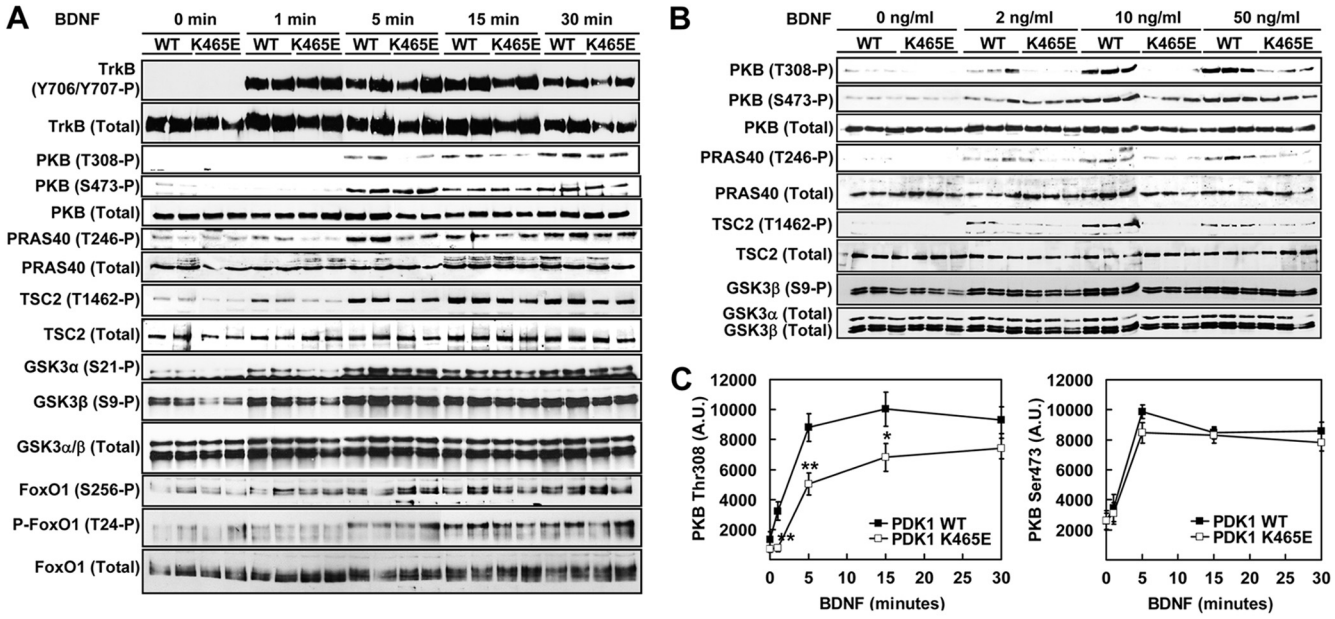

FIG 4 Deficient PKB phosphorylation and activation in PDK1$^{K465E/K465E}$ cortical neurons. (A and B) Cortical neurons from PDK1 wild-type (WT) and PDK1 K465E mouse embryos were cultured for 6 DIV and then serum starved for 4 h and either left unstimulated or stimulated with 50 ng/ml BDNF for the indicated times (A) or for 5 min with the indicated concentrations of BDNF (B). Lysates were immunoblotted with the indicated antibodies. A representative Western blot out of three independent experiments is shown, where each lane represents a sample derived from a different embryo. (C) The effect of the PDK1 K465E mutation on the phosphorylation of PKB at Thr308 and Ser473 was determined by quantitative Western blotting of cell extracts from cortical neurons stimulated as described above for panel A. Values are expressed as arbitrary units (A.U.) and are presented as the means ± standard errors of the means for protein extracts derived from three independent experiments. *, $P < 0.05$; **, $P < 0.005$ (compared with wild-type extracts, as determined by Student's *t* test).

of the neuronal processes was measured at different days *in vitro* (DIV) by scoring the length of the neurites, the number of neurites, and the number of branching points. The ability of the PDK1$^{K465E/K465E}$ embryonic cortical neurons to differentiate in culture was significantly reduced at DIV3, which was further aggravated at DIV4 (Fig. 7A). Indeed, the neurites from the PDK1$^{K465E/K465E}$ embryonic cortical neurons were 20% shorter than control PDK1$^{+/+}$ cells at DIV3; the rate of neurite outgrowth was then nearly null in the PDK1$^{K465E/K465E}$ cultures from DIV3 to DIV4, resulting in neurites that were as much as 40% shorter in the PDK1$^{K465E/K465E}$ cultures by DIV4 (Fig. 7B). To confirm than the reduced length of the PDK1$^{K465E/K465E}$ cortical neurons could not be the consequence of the reduced size of the mutant cells, we also measured the major axis of the neuronal soma and found that this was only 10% shorter in the mutant neurons (Fig. 7C). We also found that the number of neurites and branching points of the mutant neurons was similar to that of the controls, whereas the percentage of undifferentiated cells was significantly higher in the mutant cultures than in the controls (data not shown).

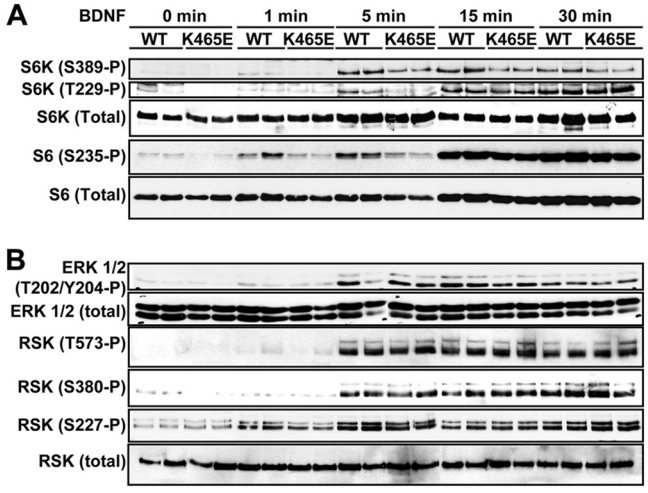

FIG 5 Analysis of S6K and RSK isoforms in PDK1$^{K465E/K465E}$ cortical neurons. Cortical neurons from two PDK1 wild-type (WT) and two PDK1 K465E mouse embryos were cultured for 6 DIV and then serum starved for 4 h and either left unstimulated or stimulated with 50 ng/ml of BDNF for the indicated times. Lysates were immunoblotted with the indicated antibodies to monitor the activation of S6K (A) and RSK (B). A representative Western blot of three independent experiments is shown.

We also took advantage of the widely used model of dissociated hippocampal neurons in culture for studying neuronal polarization (47). We determined axonogenesis during the differentiation of hippocampal primary cultures, as detected by immunocytochemistry with the specific axonal marker Tau-1 and the dendritic marker MAP2. Axon formation and growth were markedly impaired in PDK1$^{K465E/K465E}$ cells (Fig. 8A). While most of the PDK1$^{+/+}$ hippocampal neurons exhibited a differentiated axon by DIV3, the PDK1$^{K465E/K465E}$ hippocampal neurons did not reach this stage of differentiation until DIV4, and the percentage of cells exhibiting one axon was still significantly lower in the mutant cultures than the control ones, at both DIV3 and DIV4 (Fig. 8B). Moreover, the length of the axons was consistently reduced by 25% in PDK1$^{K465E/K465E}$ hippocampal neurons compared to the PDK1$^{+/+}$ controls at all the time points analyzed (Fig. 8C), while the cellular soma was only 5% shorter in the mutant hippocampal cells (data not shown). These results reveal that the interaction of

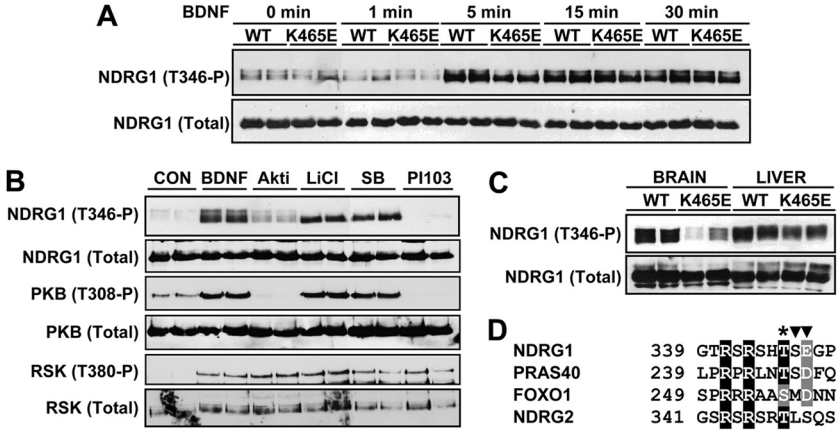

FIG 6 Analysis of SGK in PDK1$^{K465E/K465E}$ cortical neurons. (A and B) Cortical neurons from two PDK1 wild-type (WT) (A and B) and two PDK1 K465E (A) mouse embryos were cultured for 6 DIV and then serum starved for 4 h and either left untreated; stimulated with 50 ng/ml BDNF for the indicated times (A); or pretreated with the SB-216763 (3 μM), Akti-1/2 (1 μM), PI-103 (1 μM), or LiCl (10 mM) compound for 30 min, as indicated, and then stimulated with 50 ng/ml of BDNF for 5 min (B). Lysates were immunoblotted with the indicated antibodies. (C) Mouse brain and liver tissue extracts from the indicated genotypes were subjected to immunoblot analysis with the indicated antibodies. Each lane corresponds to a sample derived from a different mouse. (D) Multiple-sequence alignment of the sequence flanking the indicated phosphorylation sites in NDRG1, NDRG2, PRAS40, and FOXO1. The positions of the first amino acid aligned according to the mouse protein sequences are indicated. The black shading indicates similarity, and the gray shading indicates conservation in more than 50% of the sequences. The phosphorylated threonine or serine residues are labeled with an asterisk. Flanking residues conserved between NDRG1 and PRAS40, but not NDRG2, are marked with an arrowhead.

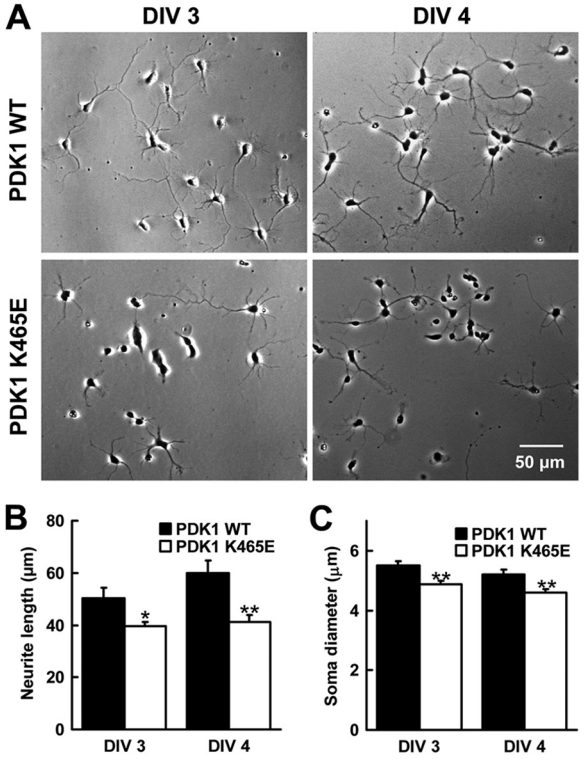

FIG 7 Deficient cortical neuritogenesis in PDK1$^{K465E/K465E}$ mice. (A) Representative micrographs of PDK1 wild-type (WT) and PDK1 K465E cortical neurons at 3 and 4 days *in vitro* (DIV). Bar, 50 μm. (B and C) The total length of the neurites (B) and the soma diameter (C) were measured on digitally acquired images. Each bar represents the mean ± standard error of the mean for 200 to 300 neurons per embryo and four embryos per genotype. *, $P < 0.05$; **, $P < 0.005$ (compared to wild-type controls, as determined by Student's *t* test).

PDK1 with phosphoinositides is required for both cortical and hippocampal neuronal morphogenesis.

To assess whether modulation of PKB activity affected neuronal differentiation directly, primary cultures of hippocampal neurons were allowed to differentiate *in vitro* for 4 days in the presence or absence of the Akti-1/2 isoform-specific inhibitor, and the axon specification and length were measured at different time points. Axon formation and growth were drastically impaired by the Akti-1/2 compound, with the percentage of cells exhibiting one differentiated axon being significantly reduced in the treated cultures compared to the control ones (Fig. 8D). Moreover, the length of the axons was also reduced in the Akti-1/2-treated hippocampal neurons to a similar extent as that observed for the PDK1$^{K465E/K465E}$ mutant cells (compare Fig. 8E and C).

In order to assess whether PKB-dependent deficient mTORC1 activation was mainly responsible for the described phenotypes, we also treated hippocampal primary cultures with the mTORC1-specific inhibitor rapamycin and found that complete inhibition of the mTORC1 pathway compromised neuronal polarization to an extent similar to that observed for the Akti-1/2-treated cells (Fig. 8D). In contrast, axonal elongation was even more severely impaired by rapamycin than by the inhibitor Akti-1/2, resulting in axons that were as much as 50% shorter than those of the untreated cells (Fig. 8E).

The tuberous sclerosis complex proteins TSC1 and TSC2 have been shown to control axon formation by modulating mTORC1 activity and the synthesis of specific proteins that are required for neuronal polarization, such as brain-specific kinase 1 (BRSK1) and BRSK2 (6). BRSK1 and BRSK2 are expressed during the differentiation of the cortex and the hippocampus, where they play fundamental roles in establishing proper neuronal polarity (7, 8). In agreement with that notion, we observed that both the BRSK1 and BRSK2 proteins were expressed at low levels in primary cultures of cortical neurons from the first day *in vitro* and that the

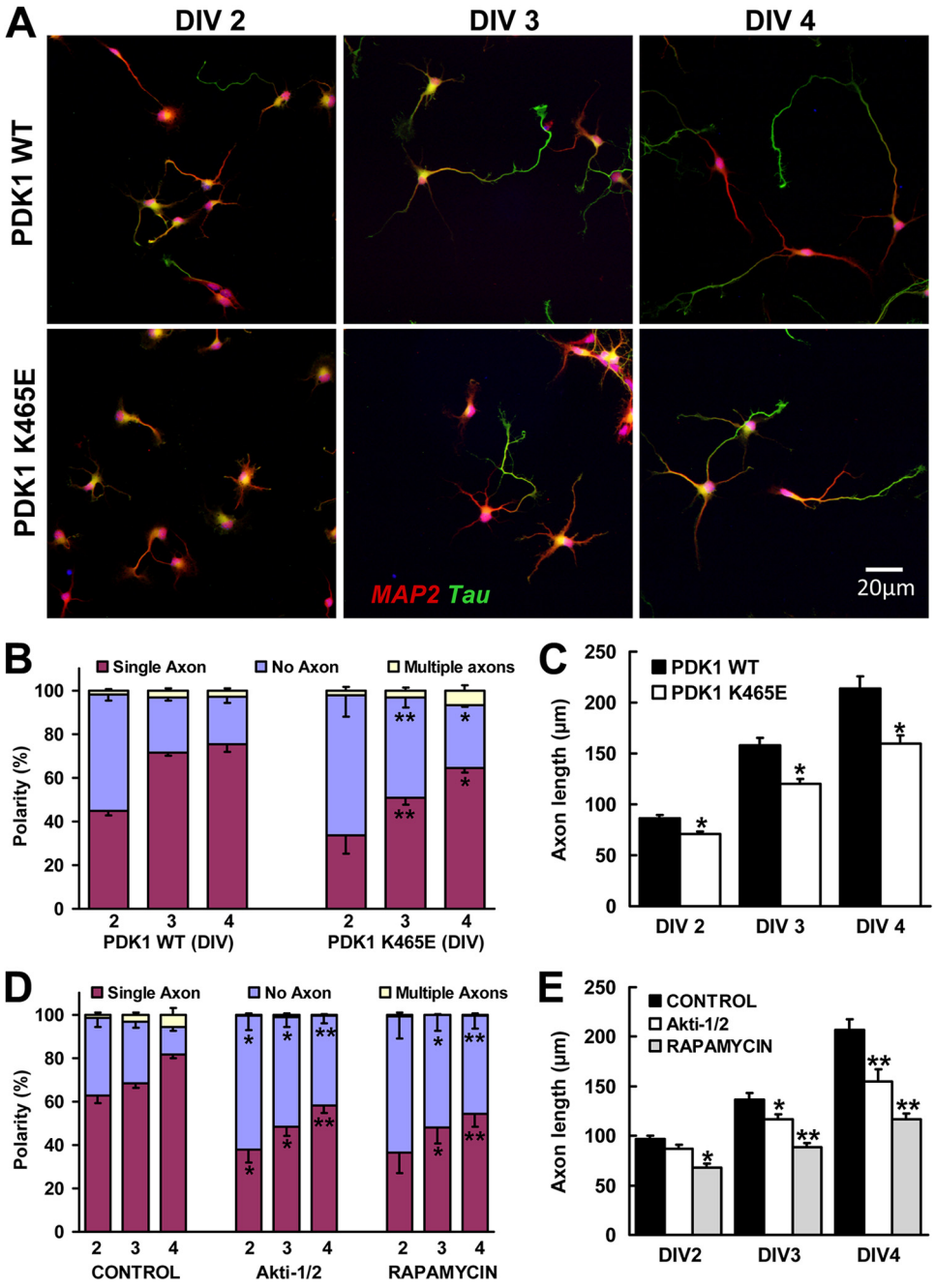

FIG 8 Deficient hippocampal axon formation and growth in PDK1$^{K465E/K465E}$ mice. (A) Representative micrographs of PDK1 wild-type (WT) and PDK1 K465E hippocampal neurons at 2, 3, and 4 days *in vitro* (DIV) stained with antibodies against the dendrite-specific marker MAP2 (red) and the specific axonal marker Tau-1 (green). Bar, 20 μm. (B to E) The percentage of polarization (B and D) and the axon elongation (C and E) of the PDK1 wild-type and the PDK1 K465E hippocampal neurons (B and C) or wild-type cells treated with the indicated inhibitors (D and E) were measured at the indicated time points. Each bar represents the mean ± standard error of the mean for 300 to 500 neurons from five different embryos per condition. *, $P < 0.05$; **, $P < 0.005$ (compared to controls, as determined by the Student *t* test).

levels of expression were then induced by day 3 *in vitro*. Strikingly, expression of the BRSK proteins was significantly reduced in the PDK1$^{K465E/K465E}$ cortical neurons from the first day in culture, which progressively recovered to nearly normal levels throughout the *in vitro* differentiation period (Fig. 9A). In agreement with this observation, BRSK1 and BRSK2 protein levels were also markedly reduced in brain extracts from PDK1$^{K465E/K465E}$ E15.5 embryos, while BRSK1 and BRSK2 protein expression was found to be similar in the adult brains of both the PDK1$^{K465E/K465E}$ and the PDK1$^{+/+}$ mice. In contrast, phosphorylation of PKB at Thr308, PRAS40 at Thr246, and TSC2 at Thr1462 was consistently reduced in the mutant protein extracts during development and in the adult (Fig. 9B). The BRSK1 expression level was also reduced in PDK1$^{K465E/K465E}$ hippocampal neurons compared to that in

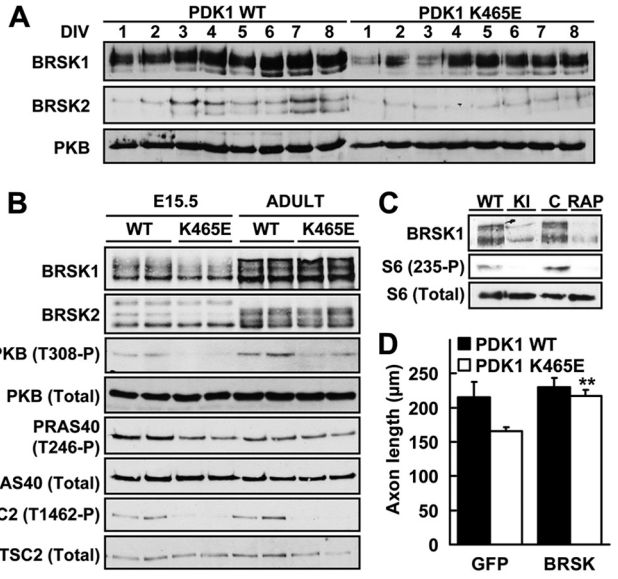

FIG 9 PDK1 promotes hippocampal axonogenesis through the PKB/mTORC1/BRSK pathway. (A) Cortical neurons from PDK1 wild-type (WT) and PDK1 K465E embryos were cultured in complete medium for the indicated times. Lysates were immunoblotted with the indicated antibodies. A representative Western blot of two independent experiments is shown. (B) Brain whole-protein extracts from PDK1 wild-type and PDK1 K465E mice of the indicated age were subjected to immunoblot analysis with the indicated antibodies. Each lane corresponds to a sample derived from a different embryo or mouse. (C) Hippocampal neurons from PDK1 wild-type and PDK1 mutant (KI) mouse embryos were cultured for 4 days in the presence (RAP) or absence (CON) of rapamycin. Lysates were immunoblotted with the indicated antibodies. A representative Western blot of three independent experiments is shown. (D) PDK1 wild-type and PDK1 K465E hippocampal cells were transfected with the indicated expression vectors at DIV2, and the axon length was determined at DIV4. Each bar represents the mean ± standard error of the mean for 100 to 200 neurons from three different embryos per condition. **, $P < 0.005$ compared to controls, as determined by the Student *t* test.

PDK1$^{+/+}$ control cells, and the treatment of these neurons with rapamycin clearly decreased the levels of BRSK1 protein (Fig. 9C). Altogether, these data suggest that the axonal phenotype observed for the PDK1$^{K465E/K465E}$ neurons is likely due to deficient PKB-mediated mTORC1 activation and blunted stimulation of BRSK expression. We tested this notion by reexpressing BRSK1 and BRSK2 in PDK1$^{K465E/K465E}$ hippocampal neurons and found that this rescued the growth deficiencies of the knock-in neurons, whereas it had little effect on the axonal elongation of wild-type cells (Fig. 9D), thereby providing strong evidence that the BRSK isoforms are key downstream targets mediating the actions of PDK1-phosphoinositide interactions in axon morphogenesis.

DISCUSSION

In the PDK1$^{K465E/K465E}$ mouse neurons, activation of PKB was partially inhibited due to an incomplete phosphorylation of PKB at the PDK1 site. Phosphorylation of the PKB Thr308 site was previously shown to be reduced 3- to 4-fold in the insulin-responsive tissues of PDK1$^{K465E/K465E}$ mice (30). We found that the impact of the PDK1 K465E mutation on PKB Thr308 phosphorylation was less severe in neuronal tissues than in insulin-responsive tissues, since BDNF-induced phosphorylation of PKB at Thr308 was reduced by only 2-fold in PDK1$^{K465E/K465E}$ cortical neurons (Fig. 4C). When the PDK1 K465E knock-in mutation was first characterized, the observation that PKB was still phosphorylated at Thr308 in the absence of a PDK1-PtdIns(3,4,5)P_3 interaction was unexpected. More recently, it was proposed that the phosphorylation of PKB at Thr308 detected in PDK1$^{K465E/K465E}$ knock-in embryonic stem (ES) cells relies on the phospho-docking site mechanism (33). It would be interesting to study whether this phospho-docking site-dependent activation of PKB operates more efficiently in neurons than in other cell types. In this regard, the activation of the docking site-dependent kinase S6K, RSK, or SGK, which occurs more slowly than the activation of PKB in several cell types, parallels the activation of PKB in neurons and reaches the maximum at 5 min of BDNF treatment.

We show that the reduced levels of PKB activation are sufficient to support the phosphorylation and inhibition of some cellular targets promoting apoptosis, such as the FOXO1 transcription factor (48) or the GSK3 kinase (49). In contrast, the reduced levels of PKB activation achieved in PDK1$^{K465E/K465E}$ neurons are rate limiting for PRAS40 and TSC2 phosphorylation. The inefficient phosphorylation of PRAS40 and TSC2 resulted in a reduced activation of mTORC1, leading to impaired phosphorylation of S6K at Thr389 within the hydrophobic motif. This most likely compromised the interaction of PDK1 with S6K, resulting in reduced S6K phosphorylation at Thr229 in the activation loop and diminished S6 protein phosphorylation, thereby explaining why the activation of a docking site-dependent kinase appears to be affected by PDK1-phosphoinositide binding. Moreover, we could bypass this requirement by stimulating mTORC1 with amino acids, which rendered normal levels of S6K and S6 protein phosphorylation in the mutant cells (data not shown).

The SGK isoforms are phosphorylated by PDK1 following the phosphorylation of their hydrophobic motif by mTORC2 (23). Because agonist-stimulated mTORC2 activation, as inferred from the levels of PKB Ser473 phosphorylation detected in the PDK1$^{K465E/K465E}$ neurons, is not affected by the PDK1 mutation, and PDK1 can phosphorylate and activate SGK in a PtdIns(3,4,5)P_3-independent manner (50), SGK1 activation was not expected to be affected in the mutant cells. In this regard, insulin-induced phosphorylation of NDRG1 at the SGK1 sites was previously shown to be preserved in the muscle and the liver of PDK1$^{K465E/K465E}$ mice (30). In contrast, phosphorylation of NDRG1 at Thr346/356/366 was reported previously to be severely impaired in several tissues of SGK1 knockout mice, including spleen, lung, liver, and muscle (41). However, we found reduced BDNF-induced phosphorylation of NDRG1 at Thr346/356/366 in PDK1$^{K465E/K465E}$ neurons. Although we failed to detect the phosphorylation of SGK1 at the Thr256 and Ser422 sites, it is unlikely that the phosphorylation of these activation sites by PDK1 or mTORC2 requires the binding of PDK1 to phosphoinositides. In contrast, we provided evidence to suggest that NDRG1 can be phosphorylated by PKB, at least in BDNF-stimulated cortical neurons. Moreover, we observed a reduced phosphorylation of NDRG1 in PDK1$^{K465E/K465E}$ brain extracts (Fig. 6C). In fact, PKB was originally shown to be capable of marginally phosphorylating the NDRG2 isoform at the Thr348 residue (41). In this regard, two of the residues in the NDRG1 sequence that conform to the specific SGK1 phosphorylation signature, namely, Ser at position $n + 1$ and Glu at position $n + 2$ C terminal from the SGK1 phosphorylation site, which were found to be deleterious to phosphorylation by PKB (51), are not conserved in the NDRG2 sequence. In contrast, PRAS40 Thr246, which is a bona fide PKB phos-

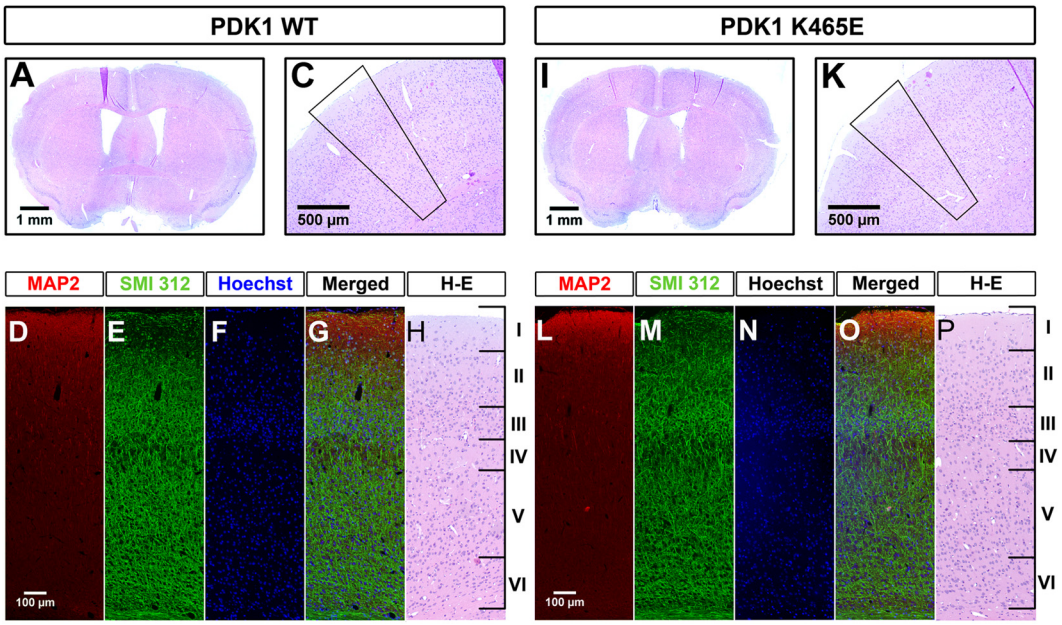

FIG 10 Normal layering and connectivity in the PDK1$^{K465E/K465E}$ adult brain. (Top) Five-micrometer-thick coronal brain sections from PDK1 wild-type (WT) (A and C) and PDK1 K465E (I and K) mice stained with hematoxylin and eosin showing the overall architecture of the rostral adult brain. (Bottom) Epifluorescence microscopy images of PDK1 wild-type (D to H) and PDK1 K465E (L to P) cortexes stained with the dendrite-specific marker MAP2 (D and L), the general axonal marker SMI-312 (E and M), and nuclear Hoechst dye (F and N). The merged signals (G and O) as well as adjacent hematoxylin-and-eosin (H-E)-stained sections (H and P) are also shown. Cortical layers are indicated on the right from I to VI.

phorylation site, possesses Ser at position $n + 1$ and Asp at position $n + 2$ C terminal from the PKB phosphorylation site (Fig. 6D).

Activation of RSK by PDK1 also relies on a phospho-docking site interaction in which the phosphorylation of the RSK hydrophobic motif is under the control of the ERK pathway. BDNF triggers the activation of both the PI3K and the ERK signaling pathways in neurons. As expected, the activation of RSK isoforms by BDNF, as monitored by the phosphorylation of the ERK site, the hydrophobic motif autophosphorylation site, and the T-loop PDK1 site, proceeded normally in the PDK1$^{K465E/K465E}$ neurons.

PDK1$^{K465E/K465E}$ mice are smaller, with a reduced cell volume resulting from deficient activation of the PKB/mTORC1/S6K signaling axis (30). The small-size phenotype is common in mice lacking different elements of this signaling network, including PKBα-deficient mice (52, 53), mTOR hypomorphic mice (54), S6K1-deficient mice (55), or S6K1 and S6K2 double knockout mice (56). In PDK1$^{K465E/K465E}$ mice, the volume of the brain was 20% reduced compared to that of the PDK1$^{+/+}$ controls. Mice lacking the PKBγ gene, which is expressed mainly in neuronal cells, displayed a selective 20 to 25% reduction of the brain size, whereas the rest of the organs analyzed were of a normal size (9, 10). In the PKBα knockout mice, a general reduction in body size that was accompanied by a proportional reduction in the sizes of different organs, including the brain, was also demonstrated (9). While the reduced brain size was attributed mainly to a decrease in the number of cells in the PKBα knockout mice, the reduced brain volume observed for the PKBγ knockout mice was proposed previously to be due mainly to the presence of smaller cells (9). Likewise, our data clearly demonstrate that the reduced brain size of the PDK1$^{K465E/K465E}$ mice is due to a reduction of the cell size, whereas the number of neurons is unaffected. It would be interesting to define whether the number and size of the neurons are specifically controlled by different PKB isoforms or whether the differences observed among the different transgenic mice could be explained in terms of whole PKB activation levels.

One salient finding derived from these studies is that in PDK1$^{K465E/K465E}$ knock-in mice, the survival responses of cortical, hippocampal, and cerebellar neurons to different neurotrophic factors are not compromised. Consistent with this conclusion, the number of neurons in the cortex and hippocampus is similar in PDK1$^{K465E/K465E}$ and control mice. PKB is a central regulator of survival and apoptosis in many neuronal types under many different stimuli. Therefore, the reduced activation of PKB observed in the PDK1$^{K465E/K465E}$ neurons might not be limiting to support the neuroprotective role of this kinase. Consistent with this, we show that the phosphorylation of some key PKB substrates that promote neuronal survival, including GSK3 and FOXO1, was not impaired in the mutant cells. Moreover, inhibition of PKBα and PKBβ, but not PKBγ, by using the Akti-1/2 compound did not compromise the neuroprotective actions of BDNF on cortical neurons deprived of serum, a situation that might resemble that of the PDK1$^{K465E/K465E}$ neurons. Because PKBγ accounts for about 40% of the total PKB protein in brain, these data suggest either that the PKBγ isoform is responsible for BDNF-mediated neuronal survival or that as little as 40% of total PKB activation is sufficient to support the survival of cortical neurons. Another scenario would be that other PDK1-activated AGC kinases different from PKB might also contribute to the neuroprotective functions of BDNF. In this regard, a specific role for SGK1 in mediating survival signals in cerebellar granule cells (11) or for RSK in cortical neurons (12) has also been proposed. Mice expressing specifically the PDK1 L155E mutation, disrupting the PDK1 substrate docking site recognition motif, in the nervous system are being generated by conditional knock-in methodologies (57). These mice will

help much in elucidating the contribution of the docking site-dependent branch of the PDK1 signaling pathway in promoting neuronal survival.

The observation that binding of PDK1 to phosphoinositides contributes to neuronal differentiation is particularly important, because deficient neuronal morphogenesis might result in a reduced ability of neurons to integrate and transmit information within the adult central nervous system, a condition which underlies many neurological and mental conditions in human disease. The differentiation of neuronal precursors onto mature neurons involves several stages that can be recapitulated *in vitro* by using dissociated mouse cortical as well as hippocampal neurons (47, 58). Here we demonstrated that the ability of cortical and hippocampal PDK1$^{K465E/K465E}$ neurons to differentiate *in vitro* was markedly impaired. This conclusion was sustained on the observations that in the PDK1$^{K465E/K465E}$ cortical neurons, the length of the neurites was significantly reduced, while axon formation and growth were diminished in the PDK1$^{K465E/K465E}$ hippocampal neurons. Interestingly, the treatment of wild-type hippocampal cultures with the PKB inhibitor Akti-1/2 or the mTORC1 inhibitor rapamycin mimicked the phenotypes of the PDK1$^{K465E/K465E}$ neurons, thereby suggesting that optimal activation of mTORC1 by PKB is required for the formation and outgrowth of the axon. We also show that the profile of expression of the BRSK isoforms throughout the *in vitro* differentiation period was blunted in PDK1$^{K465E/K465E}$ mice and that reexpression of BRSKs successfully rescued the axonal defects of the mutant hippocampal cultures. The BRSK1 and BRSK2 kinases are required for the polarization of cortical and hippocampal neurons (7, 8). Activation of BRSK isoforms by their upstream kinase LKB1 plays essential roles in neuronal polarization (8). Regulation of BRSK protein expression by TSC2/mTORC1 also influences neuronal polarity (6). Altogether, our data suggest that binding of PDK1 to phosphoinositides, acting through the PDK1/PKB/TSC2/mTORC1/BRSK pathway, is essential to efficiently transmit the extracellular signals that ultimately modulate neuronal polarization and axon outgrowth. Mice lacking both BRSK isoforms exhibited immobility and poor responsiveness and died shortly after birth. Close examination of the central nervous system demonstrated a smaller forebrain with a thinner cortex and neurons failing to form axons (7). As mentioned above, PDK1$^{K465E/K465E}$ mice are nearly viable and exhibited neither an overt phenotype nor gross abnormalities in the architecture of the central nervous system, which exhibited normal cortical layering and connectivity (Fig. 10). This finding is in agreement with the fact that the transient character of the PDK1 K465E mutation may allow the accumulation of sufficient levels of BRSK proteins in the adult tissue. However, it would be interesting to explore whether the hypomorphic reduction of PKB/mTORC1 activation, causing a delayed and/or reduced onset of BRSK protein synthesis and altered neuronal morphogenesis in the PDK1$^{K465E/K465E}$ embryo, would lead to more subtle alterations in the patterning of the central nervous system that could ultimately translate into abnormal behavioral phenotypes.

ACKNOWLEDGMENTS

We thank Dario Alessi (MRC Protein Phosphorylation Unit, Dundee, Scotland) for the mice and the antibodies. We thank Cristina Gutierrez, Mar Castillo, and Núria Barba from the Institut de Neurociencies Cell Culture, Histology, and Microscopy Facilities for technical assistance and Roser Pané, Jessica Pairada, and Nuria Riera from the SCC Estabulari de Rosegadors of the Universitat de Lleida for animal care. We also thank Arnaldo Parra and Carles Saura for their expert advice with the immunohistochemical analysis.

A Ramon y Cajal contract from the Spanish Ministerio de Educación y Ciencia supported J.R.B. T.Z. was supported by a UAB predoctoral fellowship, and X.Z. was supported by a Chinese Scholarship Council predoctoral fellowship. This work was supported by the Ministerio de Sanidad y Consumo (grant FIS-PI070101) and the Ministerio de Ciencia y Innovación (grant AES-PI10/00333).

REFERENCES

1. **Oppenheim RW.** 1989. The neurotrophic theory and naturally occurring motoneuron death. Trends Neurosci. **12**:252–255.
2. **Brunet A, Datta SR, Greenberg ME.** 2001. Transcription-dependent and -independent control of neuronal survival by the PI3K-Akt signaling pathway. Curr. Opin. Neurobiol. **11**:297–305.
3. **Datta SR, Brunet A, Greenberg ME.** 1999. Cellular survival: a play in three Akts. Genes Dev. **13**:2905–2927.
4. **Shi SH, Jan LY, Jan YN.** 2003. Hippocampal neuronal polarity specified by spatially localized mPar3/mPar6 and PI 3-kinase activity. Cell **112**:63–75.
5. **Jiang H, Guo W, Liang X, Rao Y.** 2005. Both the establishment and the maintenance of neuronal polarity require active mechanisms: critical roles of GSK-3beta and its upstream regulators. Cell **120**:123–135.
6. **Choi YJ, Di NA, Kramvis I, Meikle L, Kwiatkowski DJ, Sahin M, He X.** 2008. Tuberous sclerosis complex proteins control axon formation. Genes Dev. **22**:2485–2495.
7. **Kishi M, Pan YA, Crump JG, Sanes JR.** 2005. Mammalian SAD kinases are required for neuronal polarization. Science **307**:929–932.
8. **Barnes AP, Lilley BN, Pan YA, Plummer LJ, Powell AW, Raines AN, Sanes JR, Polleux F.** 2007. LKB1 and SAD kinases define a pathway required for the polarization of cortical neurons. Cell **129**:549–563.
9. **Easton RM, Cho H, Roovers K, Shineman DW, Mizrahi M, Forman MS, Lee VM, Szabolcs M, De Jong R, Oltersdorf T, Ludwig T, Efstratiadis A, Birnbaum MJ.** 2005. Role for Akt3/protein kinase Bgamma in attainment of normal brain size. Mol. Cell. Biol. **25**:1869–1878.
10. **Tschopp O, Yang ZZ, Brodbeck D, Dummler BA, Hemmings-Mieszczak M, Watanabe T, Michaelis T, Frahm J, Hemmings BA.** 2005. Essential role of protein kinase B gamma (PKB gamma/Akt3) in postnatal brain development but not in glucose homeostasis. Development **132**:2943–2954.
11. **Brunet A, Park J, Tran H, Hu LS, Hemmings BA, Greenberg ME.** 2001. Protein kinase SGK mediates survival signals by phosphorylating the forkhead transcription factor FKHRL1 (FOXO3a). Mol. Cell. Biol. **21**:952–965.
12. **Kharebava G, Makonchuk D, Kalita KB, Zheng JJ, Hetman M.** 2008. Requirement of 3-phosphoinositide-dependent protein kinase-1 for BDNF-mediated neuronal survival. J. Neurosci. **28**:11409–11420.
13. **Silverman E, Frodin M, Gammeltoft S, Maller JL.** 2004. Activation of p90 Rsk1 is sufficient for differentiation of PC12 cells. Mol. Cell. Biol. **24**:10573–10583.
14. **Mora A, Komander D, Van Aalten DM, Alessi DR.** 2004. PDK1, the master regulator of AGC kinase signal transduction. Semin. Cell Dev. Biol. **15**:161–170.
15. **Bayascas JR.** 2010. PDK1: the major transducer of PI 3-kinase actions. Curr. Top. Microbiol. Immunol. **346**:9–29.
16. **Pearce LR, Komander D, Alessi DR.** 2010. The nuts and bolts of AGC protein kinases. Nat. Rev. Mol. Cell Biol. **11**:9–22.
17. **Alessi DR, Pearce LR, Garcia-Martinez JM.** 2009. New insights into mTOR signaling: mTORC2 and beyond. Sci. Signal. **2**:e27. doi:10.1126/scisignal.267pe27.
18. **Hara K, Maruki Y, Long X, Yoshino K, Oshiro N, Hidayat S, Tokunaga C, Avruch J, Yonezawa K.** 2002. Raptor, a binding partner of target of rapamycin (TOR), mediates TOR action. Cell **110**:177–189.
19. **Kim DH, Sarbassov DD, Ali SM, King JE, Latek RR, Erdjument-Bromage H, Tempst P, Sabatini DM.** 2002. mTOR interacts with raptor to form a nutrient-sensitive complex that signals to the cell growth machinery. Cell **110**:163–175.
20. **Parekh D, Ziegler W, Yonezawa K, Hara K, Parker PJ.** 1999. Mammalian TOR controls one of two kinase pathways acting upon nPKCdelta and nPKCepsilon. J. Biol. Chem. **274**:34758–34764.
21. **Sarbassov DD, Guertin DA, Ali SM, Sabatini DM.** 2005. Phosphoryla-

tion and regulation of Akt/PKB by the rictor-mTOR complex. Science **307**:1098–1101.
22. **Guertin DA, Stevens DM, Thoreen CC, Burds AA, Kalaany NY, Moffat J, Brown M, Fitzgerald KJ, Sabatini DM.** 2006. Ablation in mice of the mTORC components raptor, rictor, or mLST8 reveals that mTORC2 is required for signaling to Akt-FOXO and PKCalpha, but not S6K1. Dev. Cell **11**:859–871.
23. **Garcia-Martinez JM, Alessi DR.** 2008. mTOR complex 2 (mTORC2) controls hydrophobic motif phosphorylation and activation of serum- and glucocorticoid-induced protein kinase 1 (SGK1). Biochem. J. **416**: 375–385.
24. **Biondi RM.** 2004. Phosphoinositide-dependent protein kinase 1, a sensor of protein conformation. Trends Biochem. Sci. **29**:136–142.
25. **Biondi RM, Kieloch A, Currie RA, Deak M, Alessi DR.** 2001. The PIF-binding pocket in PDK1 is essential for activation of S6K and SGK, but not PKB. EMBO J. **20**:4380–4390.
26. **Currie RA, Walker KS, Gray A, Deak M, Casamayor A, Downes CP, Cohen P, Alessi DR, Lucocq J.** 1999. Role of phosphatidylinositol 3,4,5-trisphosphate in regulating the activity and localization of 3-phosphoinositide-dependent protein kinase-1. Biochem. J. **337**(Part 3):575–583.
27. **Komander D, Fairservice A, Deak M, Kular GS, Prescott AR, Peter DC, Safrany ST, Alessi DR, Van Aalten DM.** 2004. Structural insights into the regulation of PDK1 by phosphoinositides and inositol phosphates. EMBO J. **23**:3918–3928.
28. **Alessi DR, Deak M, Casamayor A, Caudwell FB, Morrice N, Norman DG, Gaffney P, Reese CB, MacDougall CN, Harbison D, Ashworth A, Bownes M.** 1997. 3-Phosphoinositide-dependent protein kinase-1 (PDK1): structural and functional homology with the Drosophila DSTPK61 kinase. Curr. Biol. **7**:776–789.
29. **Stokoe D, Stephens LR, Copeland T, Gaffney PR, Reese CB, Painter GF, Holmes AB, McCormick F, Hawkins PT.** 1997. Dual role of phosphatidylinositol-3,4,5-trisphosphate in the activation of protein kinase B. Science **277**:567–570.
30. **Bayascas JR, Wullschleger S, Sakamoto K, Garcia-Martinez JM, Clacher C, Komander D, Van Aalten DM, Boini KM, Lang F, Lipina C, Logie L, Sutherland C, Chudek JA, van Diepen JA, Voshol PJ, Lucocq JM, Alessi DR.** 2008. Mutation of the PDK1 PH domain inhibits protein kinase B/Akt, leading to small size and insulin resistance. Mol. Cell. Biol. **28**: 3258–3272.
31. **Waugh C, Sinclair L, Finlay D, Bayascas JR, Cantrell D.** 2009. Phosphoinositide (3,4,5)-triphosphate binding to phosphoinositide-dependent kinase 1 regulates a protein kinase B/Akt signaling threshold that dictates T-cell migration, not proliferation. Mol. Cell. Biol. **29**:5952–5962.
32. **Wullschleger S, Sakamoto K, Johnstone L, Duce S, Fleming S, Alessi DR.** 2011. How moderate changes in Akt T-loop phosphorylation impact on tumorigenesis and insulin resistance. Dis. Model. Mech. **4**:95–103.
33. **Najafov A, Shpiro N, Alessi DR.** 2012. Akt is efficiently activated by PIF-pocket- and PtdIns(3,4,5)P3-dependent mechanisms leading to resistance to PDK1 inhibitors. Biochem. J. **448**:285–295.
34. **Bayascas JR.** 2008. Dissecting the role of the 3-phosphoinositide-dependent protein kinase-1 (PDK1) signalling pathways. Cell Cycle **7**:2978–2982.
35. **Lizcano JM, Goransson O, Toth R, Deak M, Morrice NA, Boudeau J, Hawley SA, Udd L, Makela TP, Hardie DG, Alessi DR.** 2004. LKB1 is a master kinase that activates 13 kinases of the AMPK subfamily, including MARK/PAR-1. EMBO J. **23**:833–843.
36. **Rodriguez-Asiain A, Ruiz-Babot G, Romero W, Cubi R, Erazo T, Biondi RM, Bayascas JR, Aguilera J, Gomez N, Gil C, Claro E, Lizcano JM.** 2011. Brain specific kinase-1 BRSK1/SAD-B associates with lipid rafts: modulation of kinase activity by lipid environment. Biochim. Biophys. Acta **1811**:1124–1135.
37. **Collins BJ, Deak M, Arthur JS, Armit LJ, Alessi DR.** 2003. In vivo role of the PIF-binding docking site of PDK1 defined by knock-in mutation. EMBO J. **22**:4202–4211.
38. **Bradford MM.** 1976. A rapid and sensitive method for the quantitation of microgram quantities of protein utilizing the principle of protein-dye binding. Anal. Biochem. **72**:248–254.
39. **Gundersen HJ, Jensen EB.** 1987. The efficiency of systematic sampling in stereology and its prediction. J. Microsc. **147**:229–263.
40. **Anjum R, Blenis J.** 2008. The RSK family of kinases: emerging roles in cellular signalling. Nat. Rev. Mol. Cell Biol. **9**:747–758.
41. **Murray JT, Campbell DG, Morrice N, Auld GC, Shpiro N, Marquez R, Peggie M, Bain J, Bloomberg GB, Grahammer F, Lang F, Wulff P, Kuhl D, Cohen P.** 2004. Exploitation of KESTREL to identify NDRG family members as physiological substrates for SGK1 and GSK3. Biochem. J. **384**:477–488.
42. **Kalaydjieva L, Gresham D, Gooding R, Heather L, Baas F, de Jonge R, Blechschmidt K, Angelicheva D, Chandler D, Worsley P, Rosenthal A, King RH, Thomas PK.** 2000. N-myc downstream-regulated gene 1 is mutated in hereditary motor and sensory neuropathy-Lom. Am. J. Hum. Genet. **67**:47–58.
43. **Okuda T, Higashi Y, Kokame K, Tanaka C, Kondoh H, Miyata T.** 2004. Ndrg1-deficient mice exhibit a progressive demyelinating disorder of peripheral nerves. Mol. Cell. Biol. **24**:3949–3956.
44. **Mitchelmore C, Buchmann-Moller S, Rask L, West MJ, Troncoso JC, Jensen NA.** 2004. NDRG2: a novel Alzheimer's disease associated protein. Neurobiol. Dis. **16**:48–58.
45. **Yamamoto H, Kokame K, Okuda T, Nakajo Y, Yanamoto H, Miyata T.** 2011. NDRG4 protein-deficient mice exhibit spatial learning deficits and vulnerabilities to cerebral ischemia. J. Biol. Chem. **286**:26158–26165.
46. **Swiech L, Perycz M, Malik A, Jaworski J.** 2008. Role of mTOR in physiology and pathology of the nervous system. Biochim. Biophys. Acta **1784**:116–132.
47. **Dotti CG, Sullivan CA, Banker GA.** 1988. The establishment of polarity by hippocampal neurons in culture. J. Neurosci. **8**:1454–1468.
48. **Tran H, Brunet A, Griffith EC, Greenberg ME.** 2003. The many forks in FOXO's road. Sci. STKE **2003**:RE5. doi:10.1126/stke.2003.172.re5.
49. **Cole AR.** 2012. GSK3 as a sensor determining cell fate in the brain. Front. Mol. Neurosci. **5**:4. doi:10.3389/fnmol.2012.00004.
50. **Kobayashi T, Cohen P.** 1999. Activation of serum- and glucocorticoid-regulated protein kinase by agonists that activate phosphatidylinositide 3-kinase is mediated by 3-phosphoinositide-dependent protein kinase-1 (PDK1) and PDK2. Biochem. J. **339**(Part 2):319–328.
51. **Murray JT, Cummings LA, Bloomberg GB, Cohen P.** 2005. Identification of different specificity requirements between SGK1 and PKBalpha. FEBS Lett. **579**:991–994.
52. **Cho H, Thorvaldsen JL, Chu Q, Feng F, Birnbaum MJ.** 2001. Akt1/PKBalpha is required for normal growth but dispensable for maintenance of glucose homeostasis in mice. J. Biol. Chem. **276**:38349–38352.
53. **Chen WS, Xu PZ, Gottlob K, Chen ML, Sokol K, Shiyanova T, Roninson I, Weng W, Suzuki R, Tobe K, Kadowaki T, Hay N.** 2001. Growth retardation and increased apoptosis in mice with homozygous disruption of the Akt1 gene. Genes Dev. **15**:2203–2208.
54. **Zhang S, Readinger JA, DuBois W, Janka-Junttila M, Robinson R, Pruitt M, Bliskovsky V, Wu JZ, Sakakibara K, Patel J, Parent CA, Tessarollo L, Schwartzberg PL, Mock BA.** 2011. Constitutive reductions in mTOR alter cell size, immune cell development, and antibody production. Blood **117**:1228–1238.
55. **Shima H, Pende M, Chen Y, Fumagalli S, Thomas G, Kozma SC.** 1998. Disruption of the p70(s6k)/p85(s6k) gene reveals a small mouse phenotype and a new functional S6 kinase. EMBO J. **17**:6649–6659.
56. **Pende M, Um SH, Mieulet V, Sticker M, Goss VL, Mestan J, Mueller M, Fumagalli S, Kozma SC, Thomas G.** 2004. S6K1(−/−)/S6K2(−/−) mice exhibit perinatal lethality and rapamycin-sensitive 5′-terminal oligopyrimidine mRNA translation and reveal a mitogen-activated protein kinase-dependent S6 kinase pathway. Mol. Cell. Biol. **24**:3112–3124.
57. **Bayascas JR, Sakamoto K, Armit L, Arthur JS, Alessi DR.** 2006. Evaluation of approaches to generation of tissue-specific knock-in mice. J. Biol. Chem. **281**:28772–28781.
58. **Craig AM, Banker G.** 1994. Neuronal polarity. Annu. Rev. Neurosci. **17**:267–310.